Design of High Sensitivity, High Resolution Compact Single Photon Imaging Devices for Small Animal and Dedicated Breast Imaging

Mark F. Smith, *Member, IEEE*, Stan Majewski, Steven R. Meikle, Andrew G. Weisenberger, Vladimir Popov, Randolph F. Wojcik

Abstract— **Imaging the biodistribution of single photon emitting radiotracers in small animals and in the breast with high resolution and high sensitivity is an important challenge. Recent work has shown that single photon emission computed tomography (SPECT) imaging of small objects with coded aperture collimators and iterative image reconstruction may provide an order of magnitude increase in sensitivity yet maintain high spatial resolution. We propose a new system design with compact detectors for single photon small animal and breast imaging. Key features are 1) multipinhole masks for improved sensitivity, 2) pixellated NaI(Tl) scintillator arrays with small crystals for high resolution and 3) flat panel or flangeless compact position sensitive photomultiplier tubes. Analyses for a small animal device with four 10 cm x 20 cm detectors and 1.5 mm detector resolution show that 0.9-1.3 mm resolution in image space could be achieved with high sensitivity for pinholes with 0.5-0.8 mm effective diameters. A design for a breast imager incorporates larger multipinhole masks, 20 cm x 20 cm pixellated detectors and lower magnification. Predicted image resolution in the center of the field of view is 1.9 mm for 0.8 mm pinholes. Additional modeling, iterative image reconstruction tests and device component tests are desirable to optimize device specifications prior to detector construction.**

I. Introduction

The design of high sensitivity, high resolution detectors for single photon imaging in biomedicine is an important challenge. One area where such detectors would be beneficial is functional small animal imaging, where potential applications include investigations of metabolism, tissue viability and receptor and gene expression. Longitudinal *in vivo* studies with single photon-emitting radiopharmaceuticals with these detectors would valuable in drug discovery and development. Detectors with high resolution and high sensitivity are also of great interest for human studies of organs such as the breast, where increased uptake of single photon tracers such as Tc-99m sestamibi has been reported in carcinomas [1].

Pinhole single photon emission computed tomography (SPECT) has been investigated for small animal imaging due to its potential for high resolution imaging achieved through object magnification Single pinhole imaging for small animals has been investigated by many research groups [2-11] and pinhole collimation has been used with pixellated detectors in a commercially available system [12]. Pinhole SPECT and PET for high resolution small animal imaging have recently been reviewed [13].

Multiple pinhole coded aperture systems have been studied for brain imaging [14, 15] and are being further considered for high resolution imaging of small objects [16] and small animals [17, 18]. A multipinhole, focused collimator has been proposed for small animal brain imaging [19]. Three-dimensional image reconstruction for multiple pinhole and coded aperture imaging with overlapping projection data is a formidable problem.

The same features that make pinhole collimation attractive for small animal imaging also apply to scintimammographic imaging, though there has been less research for this application. There have been initial studies of pinhole collimation for high resolution planar scintimammography [20] and tomographic breast imaging [21].

There are several challenges in the design of high sensitivity, high resolution compact detectors for small animal and dedicated breast imaging. In this contribution we will investigate tradeoffs between sensitivity and resolution in pinhole aperture design and between image resolution and object magnification in choosing the focal length for pinhole collimation. A methodology for deciding the placement of pinholes in a multipinhole mask will be presented. A design for compact, pixellated detectors will be developed, with attention given to the scintillator material, crystal size, overall array size, light guides, photomultiplier tubes and data acquisition system. Though small animal and breast imaging applications are considered, imaging device design for small animal imaging will be developed more fully.

M. F. Smith (telephone 757-269-5539, e-mail: mfsmith@jlab.org), S. Majewski, A. G. Weisenberger, V. Popov and R. F. Wojcik are with the Thomas Jefferson National Accelerator Facility (Jefferson Lab), Newport News, VA 23606 USA.

S. R. Meikle is with the Department of PET and Nuclear Medicine, Royal Prince Alfred Hospital, Sydney, Australia.

The Southeastern Universities Research Association (SURA) operates the Thomas Jefferson National Accelerator Facility for the United States Department of Energy under contract DE-AC05-84ER40150.

II. Imaging System Design

A. Multipinhole Mask Design and Detector Configuration

1) Initial Designs for Small Animal and Breast Imaging

The resolution and sensitivity of a small animal or dedicated breast imaging device built with a multipinhole array are dependent on several factors, including the pinhole size, the distance of the pinholes or array openings from the object and the size of the detector array. Estimates of design tradeoffs can be made using formulas developed for single pinhole imaging [22] and generalized to the multipinhole case. For pinhole SPECT the resolution from tomographic reconstruction in image space is approximately the same as that derived from planar image analysis and a similar result is expected for multipinhole single photon tomography.

Plots of resolution in image space were made as a function of object magnification and different pinhole sizes for a detector with 1.5 mm resolution (Figure 1). For small animal imaging a design goal of 1.25 mm image resolution can be achieved for magnifications less than 4 for pinhole diameters less than 0.9 mm (Figure 1a). A 15 cm x 20 cm detector would be suitable for imaging multiple, non-overlapping views of a mouse brain with this magnification, for example. Due to the larger size of the breast and a desire to limit the breast detector size to 20 cm x 20 cm, magnification cannot be as great as for small animals. This leads to a more modest target image resolution, on the order of 2 mm (Figure 1b).

Initial estimates of system sensitivity and resolution were made for prototype devices with four detectors (Figure 2). For the small animal device the multipinhole masks were 3.5 cm from the axis of rotation (AOR) and 2.9 cm wide in transaxial slices. They extended axially so that entire animal could be imaged on a 10 cm wide x 20 cm long scintillator array. Each 2.9 x 2.9 cm square area of the mask contained 100 randomly spaced pinholes. The focal length was 8.5 cm for an image magnification factor of 2.4. Sensitivity calculations assumed that a point source on the axis of rotation was imaged through 100 pinholes in each of the four masks. The modeling showed that image resolutions between 0.9 and 1.3 mm could be achieved with high sensitivity for effective pinhole diameters between 0.5 and 0.8 mm (Figure 3a).

For dedicated breast imaging larger multipinhole masks (15 cm x 15 cm) and detector heads (20 cm x 20 cm) are proposed. If the masks are located 7.5 cm from the axis of rotation, forming a square around the breast, and the detector is 16.5 cm from the axis of rotation, then magnification for a point on the AOR is 1.2. With 0.8 mm pinholes the predicted resolution on the AOR is 1.9 mm (Figure 1b) and geometric sensitivity on the AOR is 2.2% for the same pinhole density as the small animal device (Figure 3b).

Depth of interaction effects may degrade image resolution, though for the small animal device the maximum angle from normal incidence is 22.5 degrees in transaxial planes. The detectors do not completely surround the animal or breast and will be rotated for complete angular sampling. Multiplexing of images on the detector will affect signal-to-noise ratios and reconstructed image resolution and needs to be investigated.

2) Refined Design for Small Animal Imaging

The target organ for our small animal imaging application is the mouse brain, which can be modeled as a 12 mm long, 8 mm diameter cylinder. Sensitivity is a key consideration and so a new configuration for small animal imaging was designed with the center of a 3 mm diameter cylindrical mouse burrow located 2 cm from the multipinhole mask (Figure 4). The focal length is 7 cm and so magnification would be 3.5 for a point on the center of rotation in the center of the burrow. A target image resolution of approximately 1 mm can be achieved with a pinhole diameter of 0.7 mm (Figures 1, 5). This proposed system would have 2 detectors 180 degrees opposed, but because the pinhole masks are closer to the small animal, sensitivity would be greater than for the 4 detector configuration of Figure 2a.

The placement of the pinholes on the aperture mask was determined by specifying the locations of the magnified brain images on the detector, then backprojecting to find the pinhole center positions on the mask. For pinhole spacing of 12 mm axially and 7 mm transaxially there will no overlap of brain images on the detector. This spacing corresponds to a 55 pinhole configuration for a 4.8 cm x 14 cm multipinhole mask (Figure 6c). With a denser 127 pinhole mask there will be brain image overlap (Figure 7a). The masks are 5 mm thick and designed for Tc-99m imaging.

Iterative reconstructions will be performed using projection data from numerical simulations and from experimental acquisitions for the pinhole masks of Figure 6 in order to evaluate contrast and signal-to-noise. The objective will be to select a mask for which sufficient resolution can be recovered yet maintain an adequate signal-to-noise ratio in the image. The effect of overlap of body tissue activity will make brain activity estimation more difficult. The limited acceptance angle for the pinhole aperture will prevent overlap of activity from some organs at the posterior of the small animal.

B. Detector Head Design

1) Scintillator Arrays

The scintillator arrays will be made from 1 x 1 x 5 mm^3 or 1.5 x 1.5 x 10 mm^3 NaI(Tl) crystals. This new scintillator technology was very recently made available from Saint-Gobain Crystals and Detectors (formerly Bicron, Inc.). We will consult with Saint-Gobain to determine optimized scintillator array parameters. The proposed active area of the detector heads is 10 cm x 20 cm for small animal imaging and 20 cm x 20 cm for dedicated breast imaging.

2) Position Sensitive Photomultiplier Tubes (PSPMTs)

The unique detector technology to be utilized in the proposed SPECT imagers is based on an array of the new flat panel PSPMTs (which have a more uniform spatial response) if available or the presently available latest generation flangeless compact Hamamatsu R8520-00-C12 PSPMTs. The PSPMTs will be arranged in 4x8 arrays (small animal imager) or 8x8 arrays (breast imager) to form single detector heads (Figure 8). This photomultiplier technology is very

reliable and offers the opportunity to build compact, stable and robust imaging heads. The planned PSPMT spacing is 26.14 mm center-to-center with an active photocathode size of 22 mm square. Hamamatsu has indicated that a new 24 mm square version will soon be available, which will aid in imaging crystal array elements in the gap between PSPMTs.

3) Light Guides

The current solution for an optimized light guide is to use two separate optical parts to efficiently collect light from any pixel in the scintillator array. A flat "spreader" window is 4.5 mm thick and facilitates the spreading of the scintillation light cones away from dead regions along crack lines between the PSPMTs. The optical trapezoid light collectors are 4.5 mm thick and have 26.14 mm square input size (physical size of the PSPMT) and a 21 mm square output side to couple to the PMT window to match the photocathode size. The trapezoids direct light from the pixels placed above dead-edge regions between PSPMTs towards PSPMT centers. In preliminary tests this simple light guide arrangement produced very uniform response across the detector surface.

4) Advanced Detector Acquisition System

The detector will be operated with a high-rate data acquisition system built at Jefferson Lab and interfaced via high speed Ethernet to a desktop computer running reconstruction and imaging software. User interface and image display will be handled by control software developed with the Kmax 7.0 package (Sparrow Corporation, Starkville, MS) installed on an Apple Macintosh G4 computer.

For each detector head we will use a custom-designed electronically truncated centroid readout method to facilitate the digitization of the anode charge pulses from the cross-wired anodes of the PSPMTs. The R8520-00-C12 PSPMTs have 6(x)x6(y) anode wire readout. Jefferson Lab, in collaboration with Sparrow, has been developing a high performance fast VME-based data acquisition system using a Motorola MVME2700-1431 VME 366MHz G3 CPU. The analog channels of the detector are converted using the CAEN Inc. (Viareggio, Italy) V785 32 channel ADC VME board, which is able to sample all channels simultaneously with 12 bit resolution at a conversion rate of 6 microseconds. The VME CPU manages the data processing and provides image data to the Macintosh workstation. A schematic diagram of the data acquisition system is displayed in Figure 9.

III. Conclusions

A new design has been proposed for high sensitivity, high resolution detector systems for single photon small animal and breast imaging. Additional modeling, iterative image reconstruction tests and device component tests are desirable to optimize device specifications prior to detector construction.

IV. References

[1] I. Khalkhali, J. Cutrone, I. Mena, L. Diggles, R. Venegas, H. Vargas, B. Jackson, and S. Klein, "Technetium-99m-sestamibi scintimammography of breast lesions: clinical and pathological follow-up," *J. Nucl. Med.*, vol. 36, pp. 1784 -1789, 1995.

[2] S.-E. Strand, M. Ivanovic, K. Erlandsson, D. Franceschi, T. Button, K. Sjogren, and D. A. Weber, "Small animal imaging with pinhole single-photon emission computed tomography," *Cancer*, vol. 73 (suppl), pp. 981-984, 1994.

[3] D. A. Weber, M. Ivanovic, D. Franceschi, S.-E. Strand, K. Erlandsson, M. Franceschi, H. L. Atkins, J. A. Coderre, H. Susskind, T. Button, and K. Ljunggren, "Pinhole SPECT: an approach to *in vivo* high resolution SPECT imaging in small laboratory animals," *J. Nucl. Med.*, vol. 35, pp. 342-348, 1994.

[4] R. J. Jaszczak, J. Li, H. Wang, M. R. Zalutsky, and R. E. Coleman, "Pinhole collimation for ultra-high-resolution, small-field-of-view SPECT," *Phys. Med. Biol.*, vol. 39, pp. 425-437, 1994.

[5] K. Ishizu, T. Mukai, Y. Yonekura, M. Pagani, T. Fujita, Y. Magata, S. Nishizawa, N. Tamaki, H. Shibasaki, and J. Konishi, "Ultra-high resolution SPECT system using four pinhole collimators for small animal studies," *J. Nucl. Med.*, vol. 36, pp. 2282-2287, 1995.

[6] K. Ogawa, T. Kawade, K. Nakamura, A. Kubo, and T. Ichihara, "Ultra high resolution pinhole SPECT for small animal study," *IEEE Trans. Nucl. Sci.*, vol. 45, pp. 3122-3126, 1998.

[7] M. C. Wu, H. R. Tang, J. W. O'Connell, D. W. Gao, A. Ido, A. J. Da Silva, K. Iwata, B. H. Hasegawa, and M. W. Dae, "An ultra high resolution ECG-gated myocardial imaging system for small animals," *IEEE Trans. Nucl. Sci.*, vol. 46, pp. 1199-1202, 1999.

[8] N. Schramm, A. Wirrwar, F. Sonnenberg, and H. Halling, "Compact high resolution detector for small animal SPECT," *IEEE Trans. Nucl. Sci.*, vol. 47, pp. 1163-1167, 2000.

[9] B. M. W. Tsui, Y. Wang, E. C. Frey, and D. E. Wessell, "Application of an ultra high-resolution pinhole SPECT system based on a conventional camera for small animal imaging," *J. Nucl. Med.*, vol. 42, pp. 54P, 2001.

[10] F. J. Beekman, D. P. McElroy, F. Berger, E. J. Hoffman, and S. R. Cherry, "Sub-millimeter resolution in ^{125}I *in vivo* imaging in mice using micro-pinholes," *J. Nucl. Med.*, vol. 42, pp. 55P, 2001.

[11] S. Tanada, T. Irie, N. Watanabe, H. Murata, H. Murayama, and Y. Sasaki, "Performance characteristic of small-animal dedicated SPECT system," *J. Nucl. Med.*, vol. 42, pp. 204P, 2001.

[12] L. R. MacDonald, B. E. Patt, J. S. Iwanczyk, B. M. W. Tsui, Y. Wang, E. C. Frey, D. E. Wessell, P. D. Acton, and H. F. Kung, "Pinhole SPECT of mice using the LumaGEM gamma camera," *IEEE Trans. Nucl. Sci.*, vol. 48, pp. 830-836, 2001.

[13] D. A. Weber and M. Ivanovic, "Ultra-high-resolution imaging of small animals: implications for preclinical and research studies," *J. Nucl. Cardiol.*, vol. 6, pp. 332-344, 1999.

[14] R. K. Rowe, J. N. Aarsvold, H. H. Barrett, J.-C. Chen, W. P. Klein, B. A. Moore, I. W. Pang, D. D. Patton, and T. A. White, "A stationary hemispherical SPECT imager for three-dimensional brain imaging," *J. Nucl. Med.*, vol. 34, pp. 474-480, 1993.

[15] M. M. Rogulski, H. B. Barber, H. H. Barrett, R. L. Shoemaker, and J. M. Woolfenden, "Ultra-high-resolution brain SPECT imaging: simulation results," *IEEE Trans. Nucl. Sci.*, vol. 40, pp. 1123-1129, 1993.

[16] D. W. Wilson, H. H. Barrett, and E. W. Clarkson, "Reconstruction of two- and three-dimensional images from synthetic-collimator data," *IEEE Trans. Med. Imaging*, vol. 19, pp. 412-422, 2000.

[17] S. R. Meikle, R. R. Fulton, S. Eberl, M. Dahlbom, K.-P. Wong, and M. J. Fulham, "An investigation of coded aperture imaging for small animal SPECT," *IEEE Trans. Nucl. Sci.*, vol. 48, pp. 816-821, 2001.

[18] D. J. Wagenaar, J. C. Engdahl, V. Simcic, E. G. Hawman, T. Mertelmeier, U. Mahmood, R. Accorsi, and R. C. Lanza, "Use of conventional gamma cameras for small animal imaging," *Conference Record of the 2000 IEEE Nuclear Science Symposium and Medical Imaging Conference*, 2000.

[19] A. V. Ochoa, L. Ploux, R. Mastrippolito, Y. Charon, P. Lanièce, L. Pinot, and L. Valentin, "An original emission tomograph for *in vivo* brain imaging of small animals," *IEEE Trans. Nucl. Sci.*, vol. 44, pp. 1533-1537, 1997.

[20] B. M. W. Tsui, D. E. Wessell, X. D. Zhao, W. T. Wang, D. P. Lewis, and E. C. Frey, "Imaging characteristics of scintimammography using parallel-hole and pinhole collimators," *IEEE Trans. Nucl. Sci.*, vol. 45, pp. 2155-2161, 1998.

[21] C. Scarfone, R. J. Jaszczak, J. Li, M. S. Soo, M. F. Smith, K. L. Greer, and R. E. Coleman, "Breast tumor imaging using incomplete circular orbit pinhole SPECT: a phantom study," *Nucl. Med. Commun.*, vol. 18, pp. 1077-1086, 1997.

[22] H. O. Anger, "Radioisotope cameras," in *Instrumentation in Nuclear Medicine*, vol. 1, G. J. Hine, Ed. New York: Academic Press, 1967, pp. 485-552.

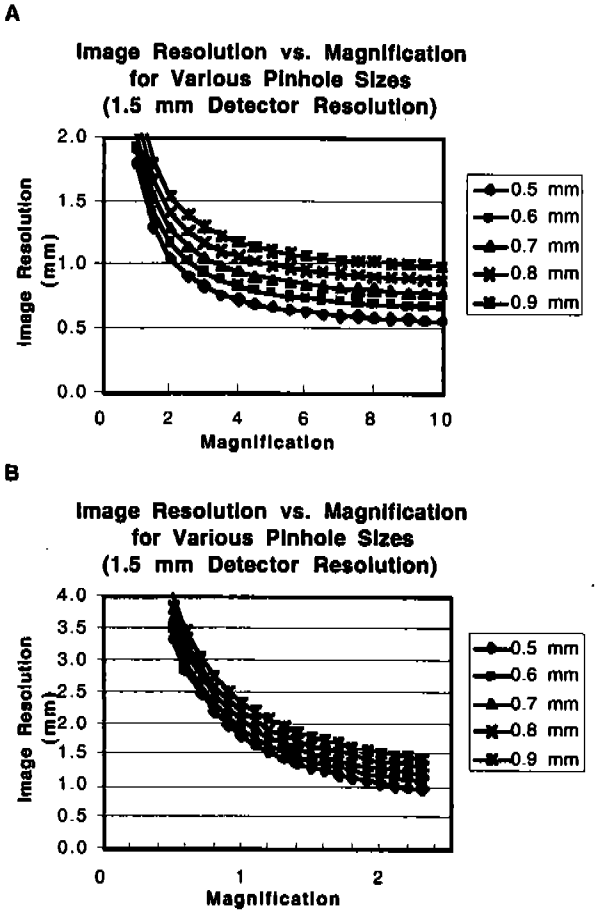

Fig. 1. Image resolution vs. magnification for various pinhole sizes. (a) Broad magnification range for small animal imaging and (b) expanded view of low magnifications for breast imaging

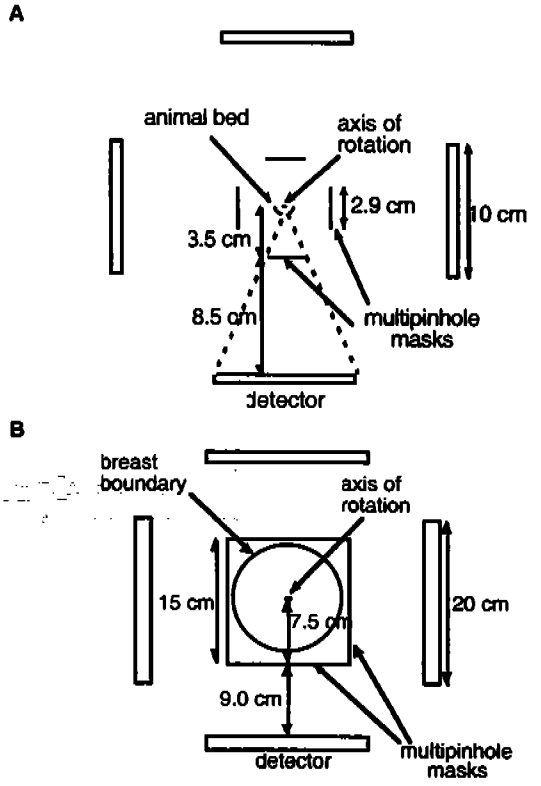

Fig. 2. Initial aperture mask and detector configurations for (a) small animal and (b) dedicated breast imaging.

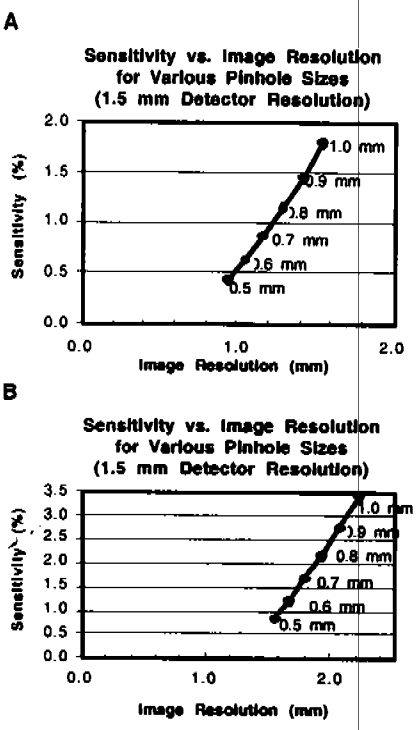

Fig. 3. Sensitivity vs. image resolution for various effective pinhole diameters (140 keV photons) for (a) small animal and (b) breast detector configurations.

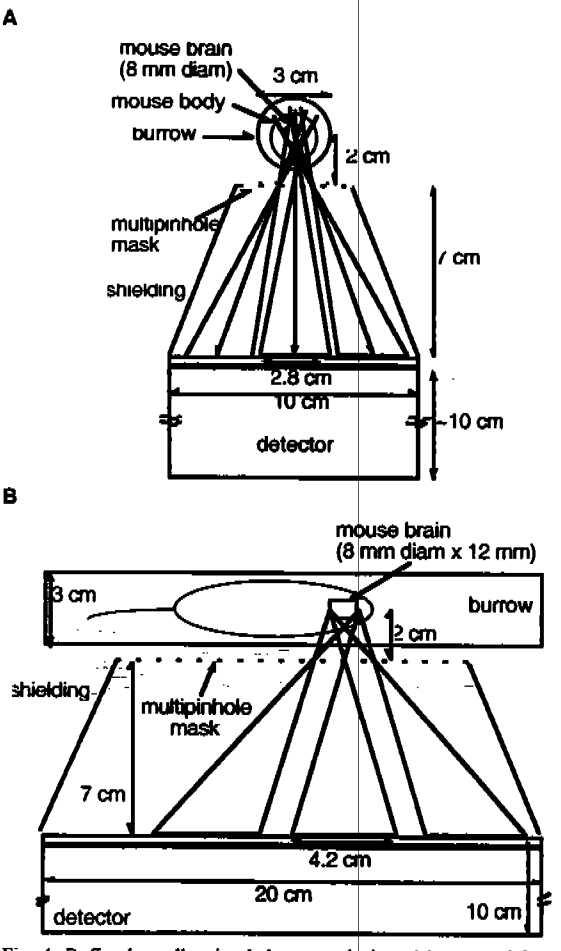

Fig. 4. Refined small animal detector design, (a) transaxial and (b) axial views.

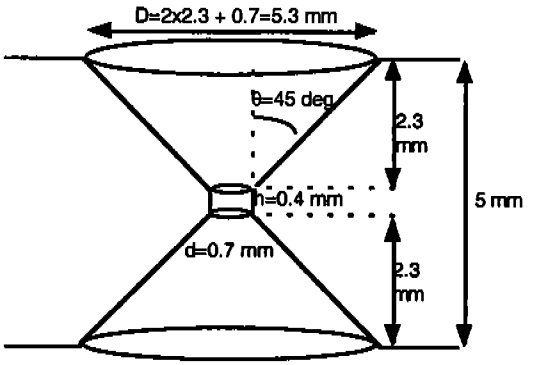

Fig. 5. Diagram of the pinhole aperture.

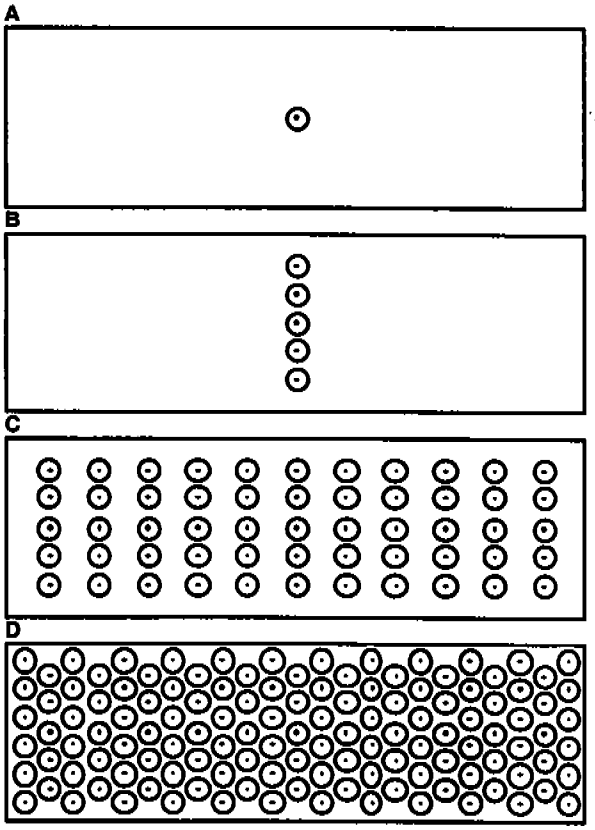

Fig. 6. Multipinhole mask designs. The centers of the apertures and the locations of the acceptance cones on the surface of the 5 mm thick masks are shown. (a) Single pinhole, (b) 5 pinhole with 7 mm spacing, (c) 55 pinhole with 12 mm axial and 7 mm transaxial spacing and (d) 127 pinhole with 6 mm between axial rows and 7 mm spacing within each axial row.

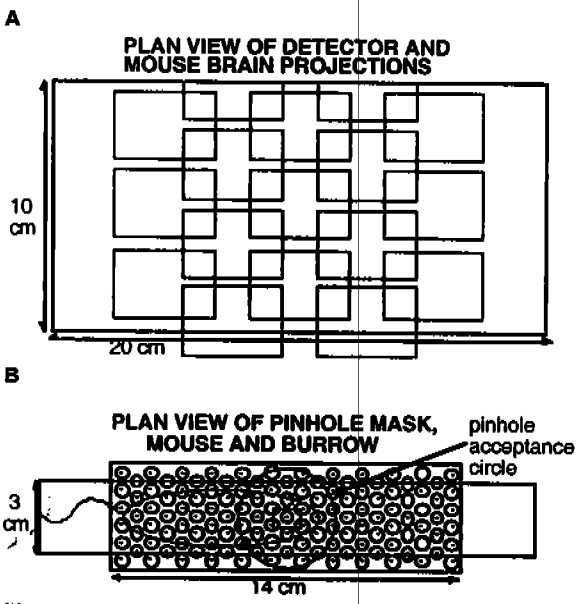

Fig. 7. (a) Plan view of mouse brain projections on the detector head for the 127 pinhole mask of Figure 6d and the mouse brain in the center of the field of view. (b) Plan view of the 127 pinhole mask, mouse burrow, mouse body outline and brain, and the pinhole acceptance circle in the plane containing the AOR. The acceptance circle is for the pinhole in the center of the mask.

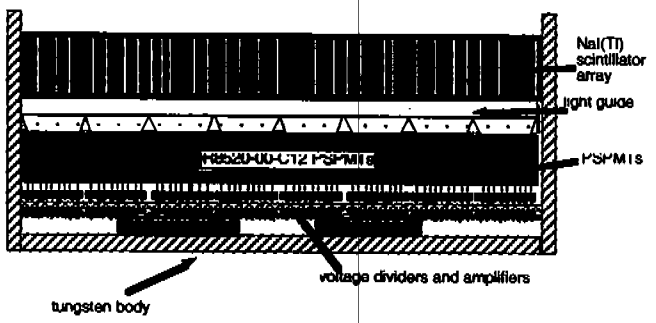

Fig. 8. Cross-section of a proposed detector head showing pixellated scintillator array, light guides, PSPMTs and front-end electronics.

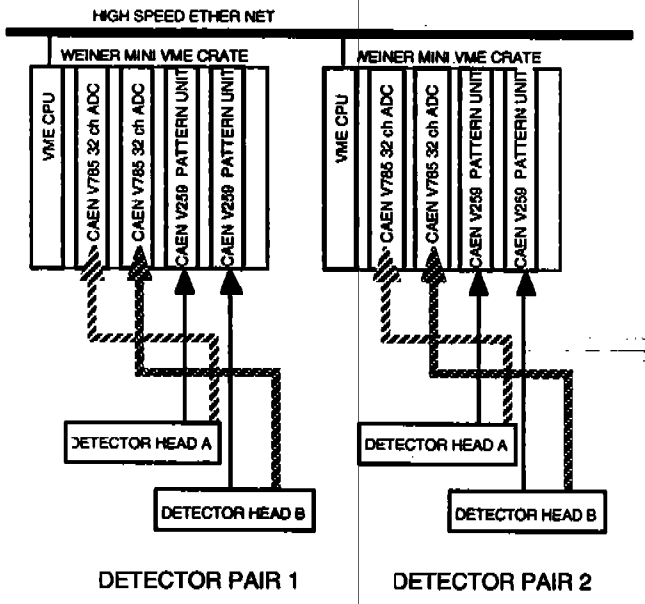

Fig. 9. Schematic diagram of the data acquisition system.